Title: Determination of glucose in human stomach cancer cell extracts and single cells by capillary electrophoresis with a micro-biosensor

Author: Xiaolei Wang Yanfang Ma Man Zhao Minfeng Zhou Yan Xiao Zifei Sun Lili Tong

PII: S0021-9673(16)31270-5
DOI: http://dx.doi.org/doi:10.1016/j.chroma.2016.09.054
Reference: CHROMA 357926

To appear in: *Journal of Chromatography A*

Received date: 15-6-2016
Revised date: 21-9-2016
Accepted date: 23-9-2016

Please cite this article as: Xiaolei Wang, Yanfang Ma, Man Zhao, Minfeng Zhou, Yan Xiao, Zifei Sun, Lili Tong, Determination of glucose in human stomach cancer cell extracts and single cells by capillary electrophoresis with a micro-biosensor, Journal of Chromatography A http://dx.doi.org/10.1016/j.chroma.2016.09.054

Determination of glucose in human stomach cancer cell extracts and single cells by capillary electrophoresis with a micro-biosensor

Xiaolei Wang,* Yanfang Ma, Man Zhao, Minfeng Zhou, Yan Xiao, Zifei Sun, Lili Tong*

College of Chemistry, Chemical Engineering and Materials Science, Shandong Normal University, Jinan 250014, PR China

***Corresponding author:** Address: 88 WenHua Dong Road, Jinan 250014, PR China; Tel: +8653186182545; Fax: +8653182615258; Email: wangxl@sdnu.edu.cn (X. Wang); findrui@gmail.com (L. Tong).

Highlights

- Glucose in single human stomach cancer cells was first determined by CE-ECD.
- CNTs and Pd nanoparticles modified micro-biosensor with CE was constructed.
- BSA and GA provided biocompatible environment and immobilized GOx firmly in the film
- The concentration of glucose was determined with high sensitivity and stability.

Abstract

Bioactive species in cells can provide information about signal transduction, cell function, and the effects of disease treatment. In this article, a novel micro-biosensor was fabricated to detect glucose in individual human stomach cancer cells (MGC80-3 cells) with capillary electrophoresis (CE). We fabricated the micro-biosensors by immobilizing a single-walled carbon nanotube-glucose oxidase (GOx)-glutaraldehyde (GA) bio-composite at the palladium nanoparticle (PdNPs) modified Pt electrode. The linear concentration of glucose ranged from 2.0 μM to 1.0 mM, with a detection limit of 0.5 μM. Using this method, the mean amount of glucose in MGC80-3 cell extracts and in single cells was 20.0 fmol and 20±6 fmol (n = 10), respectively. The micro-biosensor exhibited high sensitivity, stability, and a long operating life, which are likely due to the biocompatible environment provided by BSA and GA, and the adsorption and faster electron transfer of SWNTs and PdNPs to GOx.

Abbreviations: capillary electrophoresis (CE); human stomach cancer cell (MGC80-3 cell); single-walled carbon nanotubes (SWNTs); glucose oxidase (GOx); glutaraldehyde (GA); palladium nanoparticle (PdNPs); human hepatoma cells (HepG2); capillary electrophoresis (CE); CE with electrochemical detection (CE-ECD); ascorbic acid (AA); glutathione (GSH); dopamine(DA); microelectrodes (MEs); carbon nanotubes (CNTs); bovine serum albumin (BSA); saturated calomel electrode (SCE); Pt micro-disk electrode (PtME); PdNPs modified PtME (PdNPME); peak area (A_p); scanning electron microscopy (SEM); peak half-height ($W_{1/2}$); peak current (i_p); migration time (t_m); theoretical plate number (N); buffer concentration (C_b); relative standard deviation (RSD)

2

***Keywords*:** Glucose; Capillary electrophoresis; Electrochemical biosensor; Single-cell analysis

1. Introduction

Glucose plays an indispensable part in cell growth, nutrition and viability. Optimum glucose concentrations are important to the growing of cells for cell growth [1]. In free cytosol, glucose concentrations are usually in the millimolar range. However, glucose transport inhibitors or reduced extracellular glucose can dramatically reduce cytosolic glucose levels [2]. Glucose deprivation can negatively impact signal transduction and induce oxidative stress in human cells [3]. Determining glucose levels in individual cells can help us understand the chemical and biological functions of the cells and aid in the diagnosis and treatment of diseases. Recently, fluorescent sensors have offered an attractive approach for determining glucose concentration at the cellular level. The glucose content in a single gastric cancer cell was detected by laser-induced fluorescence [4]. Fluorescence microscopy was used to determine glucose and Ca^{2+} levels in pancreatic beta cells in real time [5]. A highly sensitive apo-GOx-modified gold nanoprobe was developed for quantitative detection of glucose in living human hepatoma cells (HepG2) [1].

Following the fabrication of the first glucose biosensor, numerous glucose sensors, such as fluorescent and electrochemical sensors, have been developed. Although fluorometry is highly sensitive, the high cost of optical instruments and the

need for chemical derivatization have led to a rise in electrochemical detection (especially amperometric detection) as the most common method. Electrochemical detection has several advantages over fluorometry, including higher sensitivity, faster response, and lower cost. However, to our knowledge, electrochemical biosensors have not been used to determine glucose levels in individual cells.

Capillary electrophoresis (CE) integrated with electrochemical detection (CE-ECD) can be used to detect analytes from femto- to atto-mole levels [6]. CE-ECD has been used to analyze ascorbic acid [7], glutathione [8], dopamine [9], histamine [10], amino acids [11,12], and glucose-6-phosphate dehydrogenase [13] in single cells. Almost all of the previously mentioned analytes were electroactive substances because carbon fiber microelectrodes (MEs) or modified MEs have typically been used in single-cell analysis. To our knowledge, CE-ECD has not been used to detect intracellular glucose. Enzymatic glucose electrochemical biosensors fabricated by the modification of glucose oxidase (GOx) on various substrates are particularly important because of their specific bioaffinity. However, endogenous electroactive substances such as DA, GSH, and AA always cause severe interference in single-cell measurements, which limits the application of enzymatic biosensors [14]. CE-based biosensors can provide accurate measurements of each individual component of a group of samples. Therefore, the development of improved micro-biosensor fabrication techniques and various modified materials will enhance sensitivity and selectivity when these novel micro-biosensors are used as the detectors of CE-ECD in single-cell assays.

Metal nanoparticles have emerged as a novel type of compound in chemistry, physics, biology, medicine, and material sciences due to their unique optical, electrical, magnetic, and catalytic properties [15]. Current research on metal nanoparticles focuses on the synthesis and application of noble metal nanoparticles such as gold, platinum, silver, palladium, and their alloys. Palladium nanoparticles (PdNPs), with their relatively high catalytic activity, have been used successfully for the measurement of nitrite [16], oxygen [17], microRNA [18], H_2O_2 [19], and glucose [20]. Meanwhile, carbon nanotubes (CNTs), which have excellent electrical conductivity and biocompatibility, are suitable candidates for improving the rate of heterogeneous electron transfer. CNTs and enzymes such as GOx are similar in size, which can facilitate their interaction [21, 22]. Furthermore, CNTs functionalization in acidic solutions creates surface binding sites such as carboxylic and hydroxyl groups, which may be favorable for biosensor applications [23, 24]. Therefore, fabrication of glucose micro-biosensors with PdNPs and CNTs may improve the detection sensitivity and reduce the response time in CE-ECD.

In this paper, a novel strategy was employed to fabricate a micro-biosensor as an electrochemical detector in CE-ECD. We fabricated the micro-biosensor by immobilizing an SWNT–GOx–glutaraldehyde biocomposite on palladium nanoparticles on a modified Pt microelectrode. The presence of glutaraldehyde (GA) and bovine serum albumin (BSA) provided a favorable biocompatible microenvironment for GOx and also played a role in reducing GOx loss. Single-wall carbon nanotubes (SWNTs) can not only interact with GOx through its binding sites

but also promote electron transfer, improve the surface area of the biosensors, and enhance catalytic activity in conjunction with PdNPs. Compared with other CE electrochemical detectors of glucose, our results demonstrated that the novel micro-biosensor exhibited better sensitivity, stability, reproducibility, and anti-interference. Glucose concentrations in both single MGC80-3 cells and cell extracts were successfully determined without complex pretreatment.

2. Experimental

2.1 Reagents and apparatus

The CE apparatus was assembled in the laboratory. The applied high voltage was provided by a 0.0 kV-30.0 kV power supply (Instrument Company of Shandong Normal University, Shandong, China). The schemes of the CE-ECD system and detection cell (Fig. 1S) were explicitly detailed in our previous work [8, 9]. Briefly, a 60-cm fused-silica capillary (25 μm ID, 375 μm OD) was set between the electrophoresis buffer reservoir and the detection buffer reservoir. The separation voltage was fixed at 18.0 kV. A CHI 832B electrochemical workstation (Shanghai, China) was used to detect glucose with CE-ECD. A glucose biosensor, a saturated calomel electrode (SCE), and a platinum wire were utilized as the working (WE), reference (RE), and auxiliary electrodes (AE), respectively.

D-glucose (>99.8%), GOx (109 U/mg) and cysteine were purchased from

Amresco (USA). SWNTs (>90%, 5–15 mm in length, <2 nm in diameter) were purified with nitric acid before use [25]. DA, AA, BSA and GA (25%) were purchased from Sigma-Aldrich Chemical Company (USA). K_2PdCl_4 was purchased from Shanghai BaoMan Biotechnology Limited Company. A phosphate buffer solution (PB, 25 mM, pH 7.4) was chosen as the running buffer for the capillary. Human stomach cancer cells (MGC80-3 cells) were purchased from the Chinese Academy of Sciences (Shanghai, China). The running buffer was used to dilute glucose stock solution (0.1 M) to the desired concentration weekly. Balanced phosphate-buffered saline (PBS, 0.2 M Na_2HPO_4 and 0.162 M NaH_2PO_4, pH 7.4) was used to suspend and clean cells. All solutions were filtered through a 0.22-μm film. Double-distilled water was used in all experimental preparations.

2.2 Fabrication of Pt micro-disk electrode and glucose micro-biosensor

The Pt micro-disk electrode (PtME) was fabricated based on our previous work [9]. A Pt wire (200 μm in diameter, 5.5 cm in length) was used. The surface of the PtME was carefully polished to a mirror-like surface on metallographical sand paper and then sonicated in ethanol and double-distilled water for 5 min. PdNPs were electrodeposited on the surface of PtME by applying a constant potential of -0.2 V (*vs.* SCE) for 15 s in a solution containing 1 mM K_2PdCl_4 and 0.5 M H_2SO_4 [26]. The electrode was removed from the solution and washed carefully using double-distilled

water. The Pd nanoparticle-modified Pt micro-disk electrode (PdNPME) was fabricated.

An enzyme solution was prepared by dissolving 10 mg of BSA and 2 mg of GOx in 0.20 mL of PB solution [27]. We thoroughly mixed a 50-μL aliquot of the enzyme solution with 10 μL of a 5% GA solution and 0.5 mg mL^{-1} SWNTs in aqueous solution (ultrasonicated for 30 min before use). The rinsed PdNPME was dipped into the enzyme solution three times for 15 s. After cross-linking at room temperature for 30 min, the glucose micro-biosensor was stored in an aqueous solution at 4 °C prior to use.

2.3 CE procedure

The CE separations were performed at room temperature (25 ± 2 °C). The capillary's injection end and detection end were placed in the electrophoresis and detection buffer reservoir, respectively. The capillary's detection end was horizontally aligned with the micro-biosensor with a three-dimensional micromanipulator. To clearly visualize the interior of the capillary, approximately 5 mm of the polyimide-coatings on both the injection and detection ends of the capillary were removed by burning. A stereomicroscope with 40× magnification was used to visualize the space and collimation between the capillary and micro-biosensor. When the equipment was set up (Fig. 1S insert), the separation voltage and the detection potential were fixed at 18.0 kV and 0.80 V, respectively. Electrokinetic injection (5.0 kV, 10 s) was used to introduce glucose samples into the capillary after a steady

current was reached. Electropherograms were recorded at 18.0 kV. The current-time curve was calculated on an electrochemical workstation.

2.4 Cell Culture

MGC80-3 cells were incubated in a 5% CO_2/95% air humidified incubator (MCO-15AC, SANYO) at 37 °C in RPMI-1640 complete medium (HyClone, Logan, USA) supplemented with 100 μg mL^{-1} streptomycin, 100 U mL^{-1} penicillin, 10% heat-inactivated fetal bovine serum, 0.3 g L^{-1} $NaHCO_3$, 0.5 g L^{-1} glucose, and 0.022 g L^{-1} sodium pyruvate. When the cells were grown to a sufficient quantity, approximately 0.25% (v/v) trypsin digestion was added into the culture dish. After the cells were suspended, trypsin was removed, and 1.5 mL of culture medium was added to the culture dish, followed by the collection of the cell suspension in a 1.5-mL centrifuge tube.

2.5 Preparation of cell extract

MGC80-3 cells were centrifuged at 1000 r min^{-1} for 5 min. The supernatant was removed carefully, and 1.0 mL of 0.2 M PBS solution was gently added with a pipette to disperse the cells. The cell concentration in the MGC80-3 cell extract was calculated to be 4.7×10^5 cell mL^{-1}. The solution was centrifuged and the supernatant was discarded. We added 1.5 mL of a 25 mM PB solution to the cells and ultrasonicated for 5 min. After the cells ruptured, the MGC80-3 cell extract solution was centrifuged at 6500 r min^{-1} for 20 min. The amount of glucose in the MGC80-3 cell extract was determined by CE-ECD.

2.6 Single-cell injection and data treatment

A homemade injector pool containing approximately 400 μL of PB buffer solution was placed on the stage of an inverted microscope, as shown in Fig. 2S(A). The capillary injection end was carefully inserted into the sample cell, and it was adjusted within the microscope field of view by the three-dimensional micromanipulator. Approximately 10 μL of suspended cells were placed in the injector pool (Fig. 2S(B)). The injection voltage was set to 3.0 kV, and a whole cell was drawn into the stripping-coating capillary tip (Fig. 2S(C)) by the electro-osmotic flow. The whole process lasted 1 to 2 min. When the cell settled at the bottom of the capillary (Fig. 2S(D)), the capillary's injection end was removed and placed into the running buffer. We applied 18.0 kV for the separation voltage, which lysed the cell during electrophoresis. Distinct dilution factors were determined from the amount of glucose in the cell samples. Therefore, the peak area (A_p) and the amount of substance standard calibration method were used for glucose quantitative analysis.

3. Results and discussion

3.1 Immobilization of GOx and SWNTs on PdNPME

The morphologies of PdNPME (Fig. 1A) and the micro-biosensor (Fig. 1B) were determined by scanning electron microscopy (SEM). The aggregates of palladium nanoparticles on the PtME surface were homogeneous and had spherical structures (diameter: 50-150 nm), which provided an increased effective electrode area for

loading some chemical functional groups, such as amines in GOx [28]. Thus, PdNPs provided excellent catalytic activity on the surface of PtME. The surface of the micro-biosensor was smooth due to the GA/BSA membrane (Fig. 1B). Many wire-like substances were homogeneously distributed within the film, which suggests that the SWNTs were evenly dispersed throughout the film. The adsorption and entrapment of GOx (4–5 nm in diameter) onto the SWNTs cannot be seen directly in the SEM images. However, it has been reported that a large number of carboxylic acid moieties (–COOH) were introduced at defect sites located at the sidewalls of SWNTs purified in nitric acid. GOx was immobilized on the SWNTs by amide linkages [29]. Therefore, SWNTs could act as highly conductive nanowires connecting nanoparticles and GOx. The schematic interfacial architecture and enzymatic process that occurs at the micro-biosensor are shown in Fig. 2. The surface morphology was smooth, which suggests that the GOx/SWNT/GA/BSA membrane was uniformly coated on the PdNPME.

The concentration of SWNTs in the film dramatically affected the sensitivity of the results (Fig. 3). Carbon nanotubes have a large surface area and fast electron transfer speed, which improves the electrode current response and decreases the reaction time. At the same time, GOx could be fixed on the surface and the inside of carbon nanotubes to maintain its activity and enhance enzyme adsorption in the film. Too many SWNTs could cause uneven distribution of the baseline noise and reduce the sensitivity of the biosensor. We used 0.5 mg/mL SWNTs for glucose detection with good sensitivity.

It has been reported that fast heterogeneous electron-transfer reactions on the detection electrodes of CE are crucial for high separation efficiency and high sensitivity [30]. If more GA and BSA were added to the enzyme solution, a thick film would be formed with an increased peak width and a longer peak shape. If less GA and BSA were used, the membrane would be too thin to be homogeneous, and the reproducibility would be significantly reduced. The presence of GA and BSA may have provided a favorable biocompatible microenvironment for GOx and also reduced enzyme loss [31]. At the optimum condition of micro-biosensor fabrication, the current-time curve was used to measure response time. The micro-biosensor would take approximately 2.5 s to achieve 95% of maximum current. The width of the electrophoretic peak half-height ($W_{1/2}$) was approximately 5.3 s under the experimental conditions. These findings suggest that the electron transfer in the membrane is fast enough to be used for amperometric detection of capillary electrophoresis.

3.2 Effects of detection parameters

The detection potential (E) directly influences the sensitivity and stability of the micro-biosensor. When E < 0.8 V, i_p was progressively enhanced and then slowly reduced. The reproducibility and stability were greater and the *S/N* ratio was largest when E was fixed at 0.8 V.

The separation voltage controls the separation process and electro-osmotic flow and thus influences the peak current (i_p), migration time (t_m), and $W_{1/2}$. When the separation potential was lower than 18.0 kV, a higher separation voltage was applied, resulting in a larger current, narrower peak, and shorter running time. This result differed from our previous work [32], as the i_p of the Au/Pt/SWNTs/chitosan micro-biosensor became smaller when higher separation voltage was used. This difference was likely due to the thinner GOx/SWNT/GA/BSA membrane fabricated by dipping compared to the GOx/SWNT/chitosan membrane fabricated by electrochemical deposition. Thus, the electron transfer speed in the GOx/SWNT/GA/BSA membrane was faster than that of the GOx/SWNT/chitosan membrane. At 18.0 kV, the peak current and theoretical plate number (N) reached their maximum values while $W_{1/2}$ reached a minimum value. Therefore, 18.0 kV was used as the separation potential throughout the remaining experiments. The noisy baselines were not noticeably enhanced under a higher separation voltage. The modified film may act as a shield against high voltage.

It is well known that the pH of the buffer is crucial for biosensor and capillary electrophoresis. The pH of the 25 mM PB buffer can influence not only the activity of biosensor but also i_p, t_m, and $W_{1/2}$. In our experiments, the buffer pH ranged from 5.5 to 8.0 when we measured the glucose content. The peak current improved dramatically from pH 5.5 to pH 7.4. As the peak current dropped from pH 7.4 to pH 8.0, i_p became largest at pH 7.4 (Table 1). This result was similar to the previous findings from Chen's group [27], where the GOx/BSA/GA-based biosensor had an

optimum pH value of 7.0. The copolymer of GA and BSA supplied a biocompatible microenvironment for GOx. Therefore, pH 7.4 was used in the following experiments.

The influence of buffer concentration (C_b) on t_m, i_p, $W_{1/2}$, and N was examined from 25 mM to 75 mM. As the concentration of pH 7.4 PB solution increased, t_m, N, and i_p declined gradually, while $W_{1/2}$ increased dramatically. We chose 25 mM as the optimal buffer concentration to obtain high sensitivity, reduce Joule heat in the capillary, and achieve the shortest analytical time.

3.3 Determination of standard glucose

Under the optimization conditions described above, the peak area (A_p) had a linear relationship with the concentration (C) and mass (n) of glucose in the range of 2.0 μM to 1.0 mM. Each concentration was tested three times. The standard calibration graph was plotted from the peak area for glucose. To improve the accuracy of the low concentration, the calibration curves were divided into two parts. The regression equation and correlation coefficient of the concentration and amount of glucose are shown in Table 2. The detection limit for glucose was 0.5 μM (S/N = 3). The mass detection limit was calculated to be 1.0 fmol, with an injection volume of 2.0 nL. The high sensitivity was attributed to the introduction of the PdNPs on the PtME and the adsorption and concentration of SWNTs to GOx. Compared with other electrochemical detectors (Table 3) (especially the Cu, Fe, Ni, and Co metal paste electrodes recently fabricated to determine glucose levels with CE-ECD), our novel

method could provide improved detection conditions, comparable detection limit and linear range with a simple electrode preparation procedure. Therefore, this method is satisfactory for detecting glucose levels in an individual cell by CE-ECD.

When ten consecutive injections of 1 mM or 5 μM glucose were performed, the relative standard deviations (RSD) of t_m and A_p were 1.4% and 3.8% and 1.8% and 5.6%, respectively, demonstrating the stability of the micro-biosensor under the operation conditions. After one month at 4°C, the peak current of glucose decayed to 84% of the original, which demonstrated that the micro-biosensor had good storage stability. The good storage stability and durability should be attributed not only to the presence of BSA and GA that provided a biocompatible environment for GOx and immobilized it firmly in the membrane but also to the adsorption of SWNTs and PdNPs to the enzyme.

3.4 Interference

It is well known that some electroactive substances, such as L-cysteine (Cys), GSH, AA, uric acid (UA), and DA often coexist with glucose in the biological matrix. Thus, the electrochemical behaviors of these five analytes at the micro-biosensor were examined (shown in Fig. 4). The results demonstrated that if this biosensor was directly used to detect complex samples by ECD, interferences from other analytes may not be negligible (the ratio was close to Ref. [27]). However, these substances do not interfere with the determination of glucose levels by CE-ECD. There were no

significant differences between the electrode responses for glucose before and after injection of a mixture of interfering species.

3.5 Determination of glucose in MGC80-3 cell extract and an individual cell

After cleaning in a 0.2 M PBS solution, the MGC80-3 cells were calculated to have a density of 4.7×10^5 cells mL^{-1}, and the cells were centrifuged again for 5 min. After discarding the supernatant, 1.5 mL of the running buffer (25 mM PB solution) was added and ultrasonicated for 5 min to obtain the extract from the MGC80-3 cells. After centrifugation for 20 min at 6500 r m^{-1}, the amount of glucose in the MGC80-3 cell extract was determined. The electropherograms of the buffer (a), cell extract (b), and 20 μM glucose (c) are shown in Fig. 5. Compared with the t_m of standard glucose, the peaks at 390 s in curves (b) and (c) could be identified as glucose in the cell extract. Using the standard calibration method, the concentration of glucose in the MGC80-3 cell extract was calculated to be 10.0 μM. Accounting for the injection volume of 2.0 nL, the mean mass of glucose in an MGC80-3 cell was 20.0 fmol $cell^{-1}$.

The electropherograms of the contents of three single MGC80-3 cells are shown in Fig. 6. These three peaks eluted at 390 s had the same migration time as standard glucose shown in Fig. 5, curve (c). Therefore, the elution peaks could be identified as glucose in single MGC80-3 cells. The large linear range for glucose standard solution, together with the reproducible peak intensity, made this method suitable to use external standardization for the quantification of glucose in single MGC80-3 cells.

The results from ten individual MGC80-3 cells are listed in Table 4. These findings demonstrated that the amounts of glucose in individual cells varied from one cell to the next. The quantities of glucose in 10 single cells ranged from 12 to 28 fmol $cell^{-1}$. The mean glucose content in an individual MGC80-3 cell was found to be 20 ± 6 fmol from the values in Table 4. This result was similar to the 20.0 fmol in the cellular extract and to previously published findings (19 ± 8.3 fmol) [4], which verified that our method was effective to determine glucose levels within single cells. Compared to fluorometric methods that usually require a complex derivatization procedure, the most obvious advantage of this method is that glucose levels in single cells can be determined directly without the influence of chemical reagents.

4. Conclusion

In this paper, a novel micro-biosensor was applied as the detector of CE-ECD to determine glucose levels. Compared with the Cu-, Ni-, and Co-modified electrodes used for determining carbohydrate levels, the micro-biosensor provided environmentally friendly detection conditions and high sensitivity. The results presented here suggest that this technique could also be developed into a useful and powerful tool for analyzing other chemical species in single cells when other types of enzymes or bioactive substances are used.

Acknowledgements

This work is financially supported by Natural Science Foundation of Shandong Province (No. ZR2014BM003); Project of Shandong Province Higher Educational Science and Technology Program (No. J14LC03), Shandong Graduate Student Novel Item (No. SDYY13012) and International Cooperation Program for Excellent Lecturers of 2015 by the Shandong Provincial Education Department.

References

[1] L. Li, F. Gao, J. Ye, Z. Chen, Q. Li, W. Gao, L. Ji, R. Zhang, B. Tang, FRET-Based biofriendly apo-GO x-modified gold nanoprobe for specific and sensitive glucose sensing and cellular imaging, Anal. Chem. 85 (2013) 9721-9727.

[2] M. Fehr, S. Lalonde, I. Lager, M. W. Wolff, W. B. Frommer, In vivo imaging of the dynamics of glucose uptake in the cytosol of COS-7 cells by fluorescent nanosensors, J. Biol. Chem. 278 (2003) 19127-19133.

[3] J. Yun, C. Rago, I. Cheong, R. Pagliarini, P. Angenendt, H. Rajagopalan, K. Schmidt, J. K. Willson, S. Markowitz, S. Zhou, Glucose deprivation contributes to the development of KRAS pathway mutations in tumor cells, Science 325 (2009) 1555-1559.

[4] F. Q. Xia and W. R. Jin, Measurement of glucose concentration in cancer cell by catalyzed-enzyme reaction, Adv. Mater. Res. 306-307 (2011) 20-24.

[5] M. T. Kaminski, S. Lenzen, S. Baltrusch, Real-time analysis of intracellular glucose and calcium in pancreatic beta cells by fluorescence microscopy, Biochim. Biophys. Acta. 1823 (2012) 1697-1707.

[6] D. J. Fischer, M. K. Hulvey, A. R. Regel, S. M. Lunte, Amperometric detection in microchip electrophoresis devices: effect of electrode material and alignment on analytical performance, Electrophoresis 30 (2009) 3324-3333.

[7] X. Wang, L. Li, Z. Li, J. Wang, H. Fu, Z. Chen, Determination of ascorbic acid in individual liver cancer cells by capillary electrophoresis with a platinum nanoparticles modified electrode, J. Electroanal. Chem. 712 (2014) 139-145.

[8] X. Wang, J. Wang, H. Fu, D. Liu, Z. Chen, Determination of glutathione in single HepG2 cells by capillary electrophoresis with reduced graphene oxide modified microelectrode, Electrophoresis 35 (2014) 3371-3378.

[9] X. Wang, Y. Ma, X. Yao, J. Wang, M. Yin, Determination of dopamine in rat less differentiated pheochromocytoma cells by capillary electrophoresis with a palladium nanoparticles microdisk electrode, RSC Adv. 3 (2013) 24605-24611.

[10] Q. Weng, F. Xia, W. Jin, Measurement of histamine in individual rat peritoneal mast cells by capillary zone electrophoresis with electrochemical detection, J. Chromatogr. B 779 (2002) 347-352.

[11] Q. Dong, X. Wang, L. Zhu, W. Jin, Method of intracellular naphthalene-2, 3-dicarboxaldehyde derivatization for analysis of amino acids in a single erythrocyte by capillary zone electrophoresis with electrochemical detection, J. Chromatogr. A 959 (2002) 269-279.

[12] W. Jin, X. Li, N. Gao, Simultaneous determination of tryptophan and glutathione in individual rat hepatocytes by capillary zone electrophoresis with electrochemical detection at a carbon fiber bundle-Au/Hg dual electrode, Anal. Chem. 75 (2003) 3859-3864.

[13.] X. Sun, W. Jin, Catalysis-electrochemical determination of zeptomole enzyme and its application for single-cell analysis, Anal. Chem. 75 (2003) 6050-6055.

[14] F. Li, Y. Feng, L. Yang, L. Li, C. Tang, B. Tang, A selective novel non-enzyme glucose amperometric biosensor based on lectin–sugar binding on thionine modified electrode, Biosens. Bioelectron. 26 (2011) 2489-2494.

[15] B. Wu, Y. Kuang, X. Zhang, J. Chen, Noble metal nanoparticles/carbon nanotubes nanohybrids: synthesis and applications, Nano Today 6 (2011) 75-90.

[16] J. H. Yang, H. Yang, S. Liu, L. Mao, Microwave-assisted synthesis graphite-supported Pd nanoparticles for detection of nitrite, Sens. Actuators. B Chem. 220 (2015) 652-658.

[17.] H. Erikson, A. Sarapuu, K. Tammeveski, J. Solla-Gullón, J. M. Feliu, Enhanced electrocatalytic activity of cubic Pd nanoparticles towards the oxygen reduction reaction in acid media, Electrochem. Commun. 13 (2011) 734-737.

[18] X. Wu, Y. Chai, R. Yuan, H. Su, J. Han, A novel label-free electrochemical microRNA biosensor using Pd nanoparticles as enhancer and linker, Analyst 138 (2013) 1060-1066.

[19] J. M. You, D. Kim, S. K. Kim, M. S. Kim, H. S. Han, S. Jeon, Novel determination of hydrogen peroxide by electrochemically reduced graphene oxide

grafted with aminothiophenol–Pd nanoparticles, Sens. Actuat. B Chem. 178 (2013) 450-457.

[20] L. M. Lu, H. B. Li, F. Qu, X. B. Zhang, G. L. Shen, R. Q. Yu, In situ synthesis of palladium nanoparticle–graphene nanohybrids and their application in nonenzymatic glucose biosensors, Biosens. Bioelectron. 26 (2011) 3500-3504.

[21] Z. Guo, P. J. Sadler, S. C. Tsang, Immobilization and visualization of DNA and proteins on carbon nanotubes, Adv. Mater. 10 (1998) 701-703.

[22] Y. Liu, M. Wang, F. Zhao, Z. Xu, S. Dong, The direct electron transfer of glucose oxidase and glucose biosensor based on carbon nanotubes/chitosan matrix, Biosens. Bioelectron. 21 (2005) 984-988.

[23] V. Mani, B. Devadas, S. M. Chen, Direct electrochemistry of glucose oxidase at electrochemically reduced graphene oxide-multiwalled carbon nanotubes hybrid material modified electrode for glucose biosensor, Biosens. Bioelectron. 41 (2013) 309-315.

[24] F. C. Vicentini, B. C. Janegitz, C. M. Brett, O. Fatibello-Filho, Tyrosinase biosensor based on a glassy carbon electrode modified with multi-walled carbon nanotubes and 1-butyl-3-methylimidazolium chloride within a dihexadecylphosphate film, Sens. Actuat. B: Chem. 188 (2013) 1101-1108.

[25] C. Niu, E. K. Sichel, R. Hoch, D. Moy, H. Tennent, High power electrochemical capacitors based on carbon nanotube electrodes, Appl. Phys. Lett. 70 (1997) 1480-1482.

[26] S. Thiagarajan, R. F. Yang and S. M. Chen, Palladium nanoparticles modified electrode for the selective detection of catecholamine neurotransmitters in presence of ascorbic acid, Bioelectrochemistry 75 (2009) 163-169.

[27] H. Wang, X. Wang, X. Zhang, X. Qin, Z. Zhao, Z. Miao, N. Huang, Q. Chen, A novel glucose biosensor based on the immobilization of glucose oxidase onto gold nanoparticles-modified Pb nanowires, Biosens. Bioelectron. 25 (2009) 142-146.

[28] Q. Zeng, J. S. Cheng, X. F. Liu, H. T. Bai, J. H. Jiang, Palladium nanoparticle/chitosan-grafted graphene nanocomposites for construction of a glucose biosensor, Biosens. Bioelectron. 26 (2011) 3456-3463.

[29] Y. Lin, F. Lu, Y. Tu, Z. Ren, Glucose biosensors based on carbon nanotube nanoelectrode ensembles, Nano lett. 4 (2004) 191-195.

[30] J. Wang, B. Tian, M. P. Chatrathi, A. Escarpa, M. Pumera, Effects of heterogeneous electron‐transfer rate on the resolution of electrophoretic separations based on microfluidics with end‐column electrochemical detection, Electrophoresis 30 (2009) 3334-3338.

[31] R. Kurita, H. Tabei, Y. Iwasaki, K. Hayashi, K. Sunagawa, O. Niwa, Biocompatible glucose sensor prepared by modifying protein and vinylferrocene monomer composite membrane, Biosens. Bioelectron. 20 (2004) 518-523.

[32] X. Wang, Y. Zhang, C. Cheng, R. Dong, J. Hao, Glucose in human serum determined by capillary electrophoresis with glucose micro-biosensor, Analyst 136 (2011) 1753-1759.

[33] Y. Du, J. Yan, W. Zhou, X. Yang, E. Wang, Direct electrochemical detection of glucose in human plasma on capillary electrophoresis microchips, Electrophoresis 25 (2004) 3853-3859.

[34] G. Chen, Y. Wang, P. Yang, Amperometric biosensor coupled to capillary electrophoresis for glucose determination, Microchim. Acta 150 (2005) 239-245.

[35] Y. Fu, L. Zhang, G. Chen, Preparation of a carbon nanotube-copper nanoparticle hybrid by chemical reduction for use in the electrochemical sensing of carbohydrates, Carbon 50 (2012) 2563-2570.

[36] R. Zhang, S. Lu, L. Zhang, G. Chen, Assembly of graphene and nickel nanoparticles on anion exchange resin microspheres for the amperometric detection of carbohydrates in combination with capillary electrophoresis, J. Chromatogr. A 1374 (2014) 261-267.

[37] Y. Lin, P. Yu, J. Hao, Y. Wang, T. Ohsaka, L. Mao, Continuous and Simultaneous Electrochemical Measurements of Glucose, Lactate, and Ascorbate in Rat Brain Following Brain Ischemia, Anal. Chem. 86 (2014) 3895-3901.

[38] P. Liang, M. Sun, P. He, L. Zhang, G. Chen, Determination of carbohydrates in honey and milk by capillary electrophoresis in combination with graphene–cobalt microsphere hybrid paste electrodes, Food Chem. 190 (2016) 64-70.

Captions

Fig. 1. SEM images of PdNPME (A) and the micro-biosensor (B); Accelerating voltage: 5000 V, Spray time: 30 s

Fig. 2. Schematic presentation of the fabricated glucose micro-biosensor.

Fig. 3. Effect of SWCNT concentration on peak current. Fused-silica capillary: 25 μm I.D. /60 cm; detection potential: 0.8 V (*vs.* SCE); running buffer: 25 mM pH 7.4 PB; injection time: 5.0 kV/10 s, detection times: 3.

Fig. 4. Electropherograms of the standard solution of interferences of DA (0.2 mM), glucose (0.6 mM), L-Cys (0.5 mM), GSH (0.5 mM), AA (1 mM), UA (0.8 mM). Other conditions as in Fig. 3.

Fig. 5. Electropherograms of PB buffer (a), cell extract (b) and 20 μM glucose (c). Other conditions as in Fig. 3.

Fig. 6. Electropherograms of PB buffer solution (a), an individual MGC80-3 cell (b), (c), (d). Other conditions as in Fig. 3.

Fig. 1.

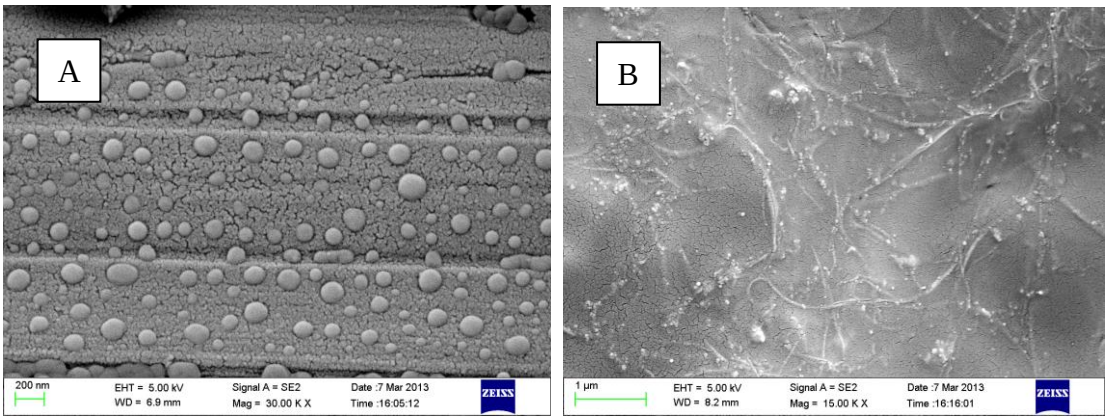

Fig.2.

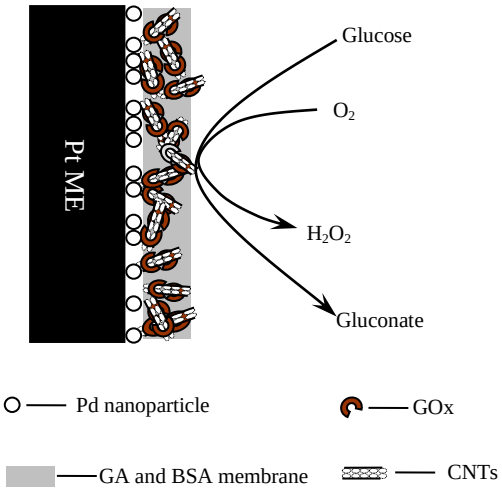

Fig. 3.

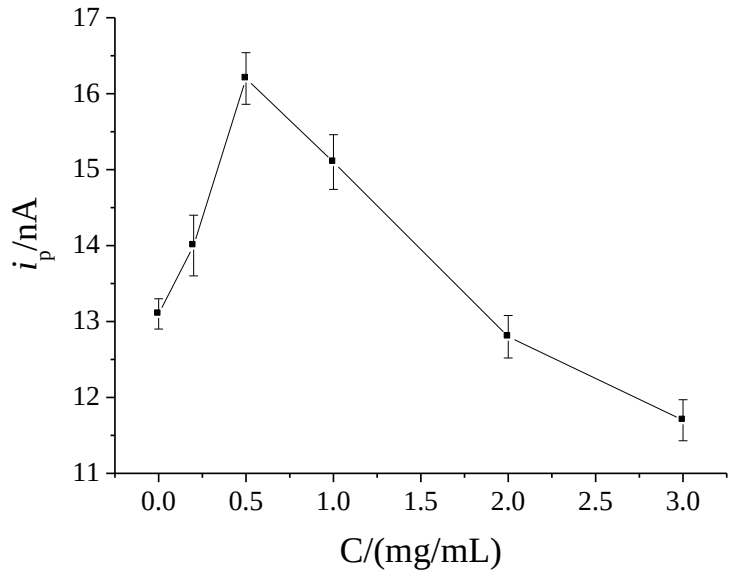

Fig. 4.

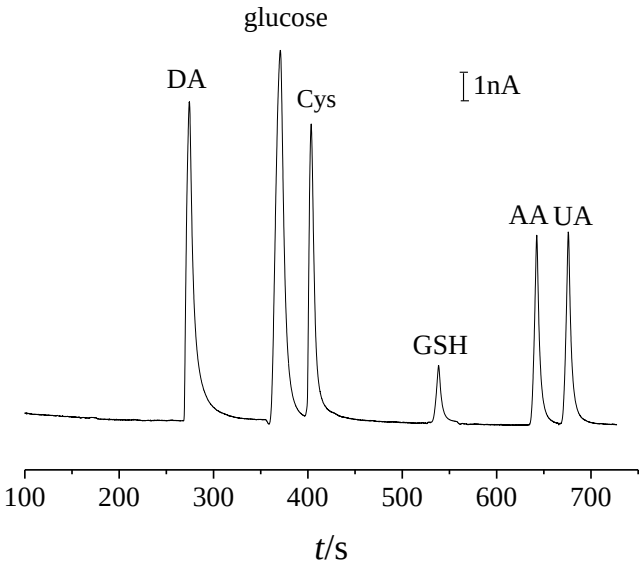

Fig. 5.

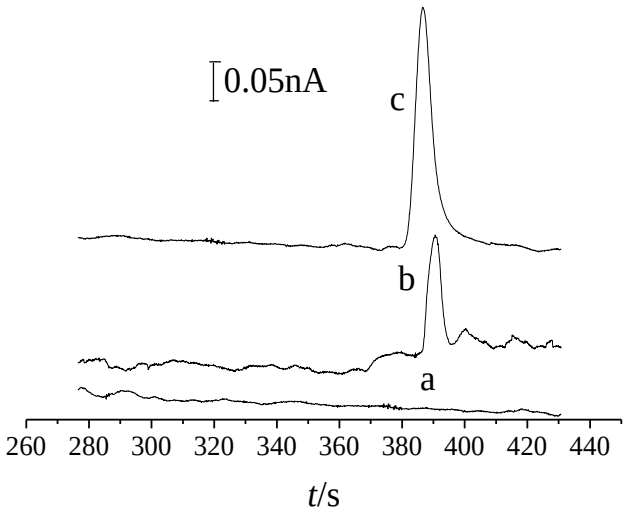

Fig. 6.

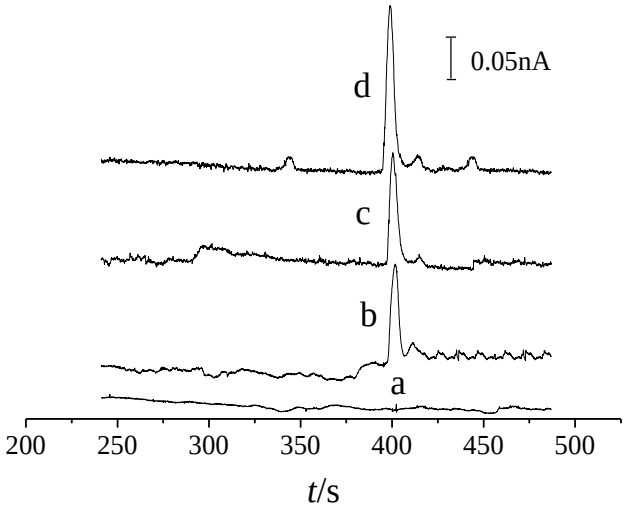

Table 1 Effect of acidity (pH) on the detection of 1 mM glucose. Other conditions as in Fig. 3.

pH	i_p/nA	t_m/s	$W_{1/2}$/s	N
5.5	13.2	352	6.2	17857
6.0	14.3	358	6.0	19723
6.5	14.9	365	5.8	21940
7.0	16.1	377	5.5	26029
7.4	17.2	398	5.3	31240
8.0	15.7	402	5.2	33109

Table 2 Analytical performance of the proposed method (n = 3)

Linearity range	Regression equation	R
60 μM to 1 mM	A_p(nC)=5.989+224.5 C(mM) A_p(nC)= 5.989+0.1123 n(pmol)	0.9970
2 μM to 80 μM	A_p(nC)=0.7487+0.2356 C(μmol/L) A_p(nC)=0.7487+0.1178 n(fmol)	0.9973

Table 3 Comparison of different biosensors for standard glucose determination

Electrodes	Linearity range	LODs（μM）	Ref
copper electrode [a]	10 μM ~1 mM	6	[32]
1-Ferrocenylethylamine and chitosan modified platinum electrode [a]	2.5 μM ~2.5 mM	1.2	[33]
Au/Pt/SWNTs/chitosan/GOx micro-biosensor [a]	5 μM ~ 1 mM	1	[31]
CNT-CuNPs hybrid paste electrode [a]	1 μM ~ 2 mM.	0.4	[34]
Graphene-NiNPs assembled anion exchange resin microspheres electrode [a]	1 μM ~ 1 mM	0.22	[35]
GDH/MG/SWNTs-modified ITO electrode [b]	0.5 mM ~ 10 mM	200	[36]
graphene–cobalt microsphere hybrid paste electrode [a]	1 μM ~ 2 mM	0.2	[37]
GOx-BSA-GA-based biosensor [a]	2 μM ~ 1 mM	0.5	This paper
[a] capillary electrophoresis; [b] microfluidic chip			

Table 4 Migration time (t_m), peak area (A_p) and amount of glucose (q) in single MGC80-3 cells

cell no.		t_m/s	A_p/nA	q/fmol
1		391	2.0	12
2		386	3.9	20
3		388	4.0	26
4		385	4.6	28
5		393	2.8	16
6		384	2.6	14
7		392	2.7	15
8		396	3.8	24
9		387	2.8	16
10		394	4.1	27